An update to this article is included at the end

Report

Current Biology

Cell-Size Control and Homeostasis in Bacteria

Graphical Abstract

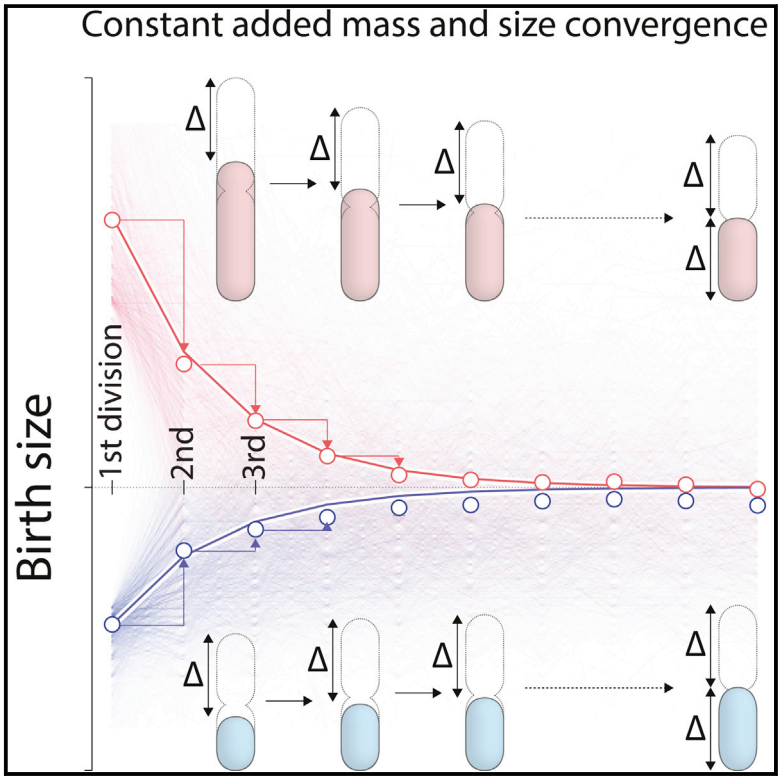

Authors

Sattar Taheri-Araghi, Serena Bradde, ..., Massimo Vergassola, Suckjoon Jun

Correspondence

massimo@physics.ucsd.edu (M.V.), suckjoon.jun@gmail.com (S.J.)

In Brief

Taheri-Araghi et al. present extensive single-cell data from Gram-negative *E. coli* and Gram-positive *B. subtilis* showing that in both cases, cells add a constant volume, irrespective of birth size, and this automatically ensures size homeostasis.

Highlights

- Individual cells show systematic deviations from the population-level growth law
- Cells sense neither space nor time but add constant mass, irrespective of birth size
- The adder principle automatically ensures size homeostasis
- All measured distributions collapse when rescaled by their respective means

Taheri-Araghi et al., 2015, Current Biology *25*, 385–391
February 2, 2015
http://dx.doi.org/10.1016/j.cub.2014.12.009

Current Biology 25, 385–391, February 2, 2015 ©2015 Elsevier Ltd All rights reserved http://dx.doi.org/10.1016/j.cub.2014.12.009

Report

Cell-Size Control and Homeostasis in Bacteria

Sattar Taheri-Araghi,[1,7] Serena Bradde,[2,7] John T. Sauls,[1] Norbert S. Hill,[3] Petra Anne Levin,[4] Johan Paulsson,[5] Massimo Vergassola,[1,*] and Suckjoon Jun[1,6,*]
[1]Department of Physics, University of California San Diego, La Jolla, CA 92093, USA
[2]Initiative for the Theoretical Sciences, The Graduate Center, City University of New York, 365 Fifth Avenue, New York, NY 10016, USA
[3]Department of Molecular & Cell Biology, University of California, Berkeley, CA 94720, USA
[4]Department of Biology, Washington University, Saint Louis, MO 63130, USA
[5]Department of Systems Biology, Harvard Medical School, Longwood, MA 02115, USA
[6]Section of Molecular Biology, Division of Biological Science, University of California San Diego, La Jolla, CA 92093, USA

Summary

How cells control their size and maintain size homeostasis is a fundamental open question. Cell-size homeostasis has been discussed in the context of two major paradigms: "sizer," in which the cell actively monitors its size and triggers the cell cycle once it reaches a critical size, and "timer," in which the cell attempts to grow for a specific amount of time before division. These paradigms, in conjunction with the "growth law" [1] and the quantitative bacterial cell-cycle model [2], inspired numerous theoretical models [3–9] and experimental investigations, from growth [10, 11] to cell cycle and size control [12–15]. However, experimental evidence involved difficult-to-verify assumptions or population-averaged data, which allowed different interpretations [1–5, 16–20] or limited conclusions [4–9]. In particular, population-averaged data and correlations are inconclusive as the averaging process masks causal effects at the cellular level. In this work, we extended a microfluidic "mother machine" [21] and monitored hundreds of thousands of Gram-negative *Escherichia coli* and Gram-positive *Bacillus subtilis* cells under a wide range of steady-state growth conditions. Our combined experimental results and quantitative analysis demonstrate that cells add a constant volume each generation, irrespective of their newborn sizes, conclusively supporting the so-called constant Δ model. This model was introduced for *E. coli* [6, 7] and recently revisited [9], but experimental evidence was limited to correlations. This "adder" principle quantitatively explains experimental data at both the population and single-cell levels, including the origin and the hierarchy of variability in the size-control mechanisms and how cells maintain size homeostasis.

[7]Co-first author
*Correspondence: massimo@physics.ucsd.edu (M.V.), suckjoon.jun@gmail.com (S.J.)

Results

At the Population Level, New Experimental Data Confirm the Growth Law

Population-level parameters derived from our single-cell data followed established patterns for microbial growth known as the growth law [1]: the average newborn cell volume $\langle v_b \rangle$ increased and the average generation time $\langle \tau_d \rangle$ decreased, respectively, as the nutrient-imposed growth rate $\langle \lambda \rangle = \langle 1/\tau_d \rangle \ln 2$ increased (newborn refers to the cells right after birth; Figure 1A). The newborn cell volume depended exponentially on the nutrient-imposed growth rate (hereafter referred to as growth rate, unless otherwise noted), $\langle v_b \rangle = A \exp(B\langle \lambda \rangle)$, in quantitative agreement with the growth law [1] (Figure 1C, red symbols and line; A is the y intercept, and B is the slope of the red line). Moreover, newborn length $\langle s_b \rangle$ and width $\langle w_b \rangle$, averaged over the entire set of individual cells in each growth condition, also showed an exponential dependence on the average growth rate $\langle \lambda \rangle$ (Figure S1A available online).

The size of individual cells also increased exponentially as $s(t) = s_b 2^{\alpha t}$ (where α is the instantaneous elongation rate), and… their width did not change significantly between birth and division (Figure S1B; [21]; hereafter, we use size and volume synonymously). The average instantaneous elongation rate was identical to the average growth rate of the population since $\langle 1/s\ ds/dt \rangle = \langle \alpha \rangle \ln 2 = \langle 1/\tau_d \rangle \ln 2 = \langle \lambda \rangle$.

At the Single-Cell Level, Individual Cells Show Systematic Deviations from the Growth Law

Individual cells, however, exhibited intrinsic variability even under constant growth conditions, and we asked whether the quantitative relationship between the average size and the average growth rate also applied at the single-cell level. For example, the SDs of the growth rate and the newborn cell size were ~15% and ~14% of their respective means (Figure 1B). Therefore, when the growth-rate distributions for two different growth conditions partially overlapped as shown in Figure 1B, individual cells in the overlap region could have had the same growth rate $\lambda = (\ln 2)/\tau_d$. Thus, if the growth rate solely defined the cell's growth physiology, individual cells with the same λ should have had on average the same size as described by the growth law $\langle v_b \rangle = A \exp(B\langle \lambda \rangle)$. We found this was not the case. For all seven growth conditions, the size versus growth rate measured from individual cells, v_b versus λ, systematically deviated from the population-level growth law (Figure 1C, blue symbols and lines versus red symbols and line). This deviation indicates that, at the single-cell level, the size of individual cells is controlled by a mechanism that is different from the growth law $\langle v_b \rangle = A \exp(B\langle \lambda \rangle)$ (see below).

Correlations of Growth and Size Parameters Contradict Both Sizer and Timer Models

The newborn cell size (s_b) and the generation time (τ_d) of individual cells were negatively correlated (Figure 1D, left), which excluded the timer model of cell-size control. Otherwise, we would have seen constant τ_d with respect to s_b. Furthermore, timer models showed instability when accounting for the

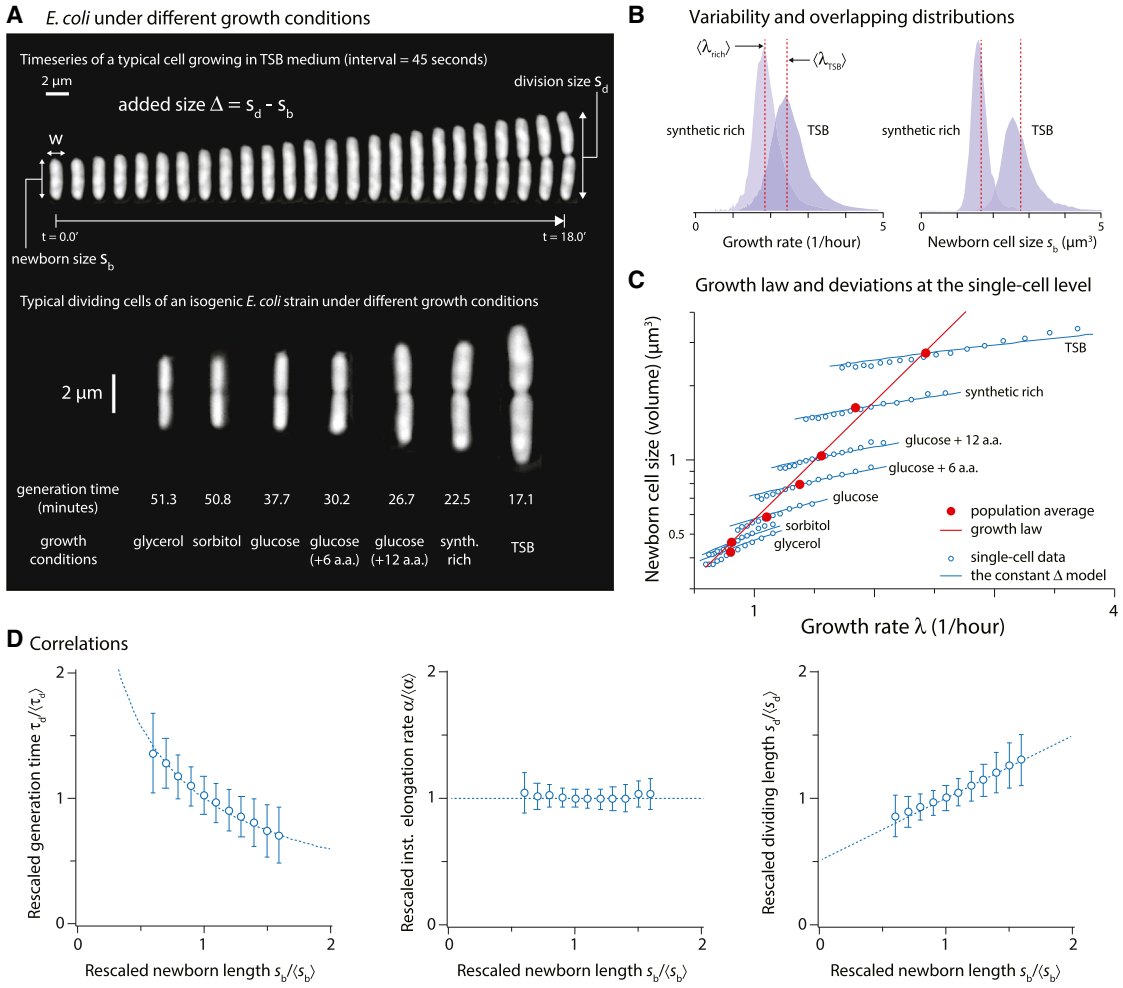

Figure 1. Growth Law at the Population Level and Systematic Deviations at the Single-Cell Level

(A) Top: time series of a typical cell growing in a nutrient-rich medium. Bottom: sample images of dividing *E. coli* cells in steady-state exponential growth at 37°C in seven different growth media.

(B) Partially overlapping distributions of the growth rate and the newborn size measured from individual cells in two different growth conditions. The vertical lines show the population average values. Cells in the overlap region can have the same growth rate or newborn cell size.

(C) Population average of single-cell measurements demonstrates exponential dependence of newborn cell volume on the average growth rate (red). However, s_b versus λ of individual cells (binned data in empty blue circles; measured by following them from birth to division) shows systematic deviations from the average growth law. Thus, although the cells in the overlap region in (B) can have the same growth rate or newborn cell size, the size of individual cells are controlled by a mechanism that is different from the growth law. Otherwise, all blue symbols would have fallen on top of the red line.

(D) Correlations between rescaled growth parameters at the single-cell level with SDs from the entire set of *E. coli* data. Left: generation time versus size at birth. Middle: elongation rate versus size at birth. Right: size at division versus size at birth. Dashed lines indicate predictions from the adder principle from this work. The first correlation falsifies the timer model, whereas the last correlation falsifies the sizer model.

See also Figure S1.

observed exponential growth of individual cells (Supplemental Information). The fact that cells born small take on average more time before they divide is in principle consistent with a sizer model. However, the strong positive correlations between the dividing size s_d and s_b (Figure 1D, right) ruled out the model because the sizer predicted that s_d should be constant.

Cells Instead Employ "Adder" Principle

Our data instead support a model in which the size added between birth and division ($\Delta = s_d - s_b$) is constant for given growth conditions. We found that, although Δ varied significantly between growth conditions and also between individual cells, Δ was on average constant irrespective of the newborn size s_b in each growth condition (Supplemental Information). In fact, the entire conditional distribution $\rho(\Delta|s_b)$ had the same shape as the nonconditional distribution $\rho(\Delta)$, and distributions of Δ from different experimental conditions collapsed onto a single curve when rescaled by their mean (Figure 2, right; Figure S2). The distribution of the size added in each generation, Δ, was thus independent of the newborn cell size.

We also confirmed the constancy of Δ in two additional *E. coli* strains from our previous work (K12 MG1655 and B/r) [21] (Figure S3) and *E. coli* size mutants (Δpgm and ftsA*) [16]. Furthermore, we also confirmed the validity of the model in the Gram-positive *B. subtilis* (Figures 2B and 2C).

The collapse of the conditional distributions in Figure 2 established the constant Δ model, or adder (as opposed to

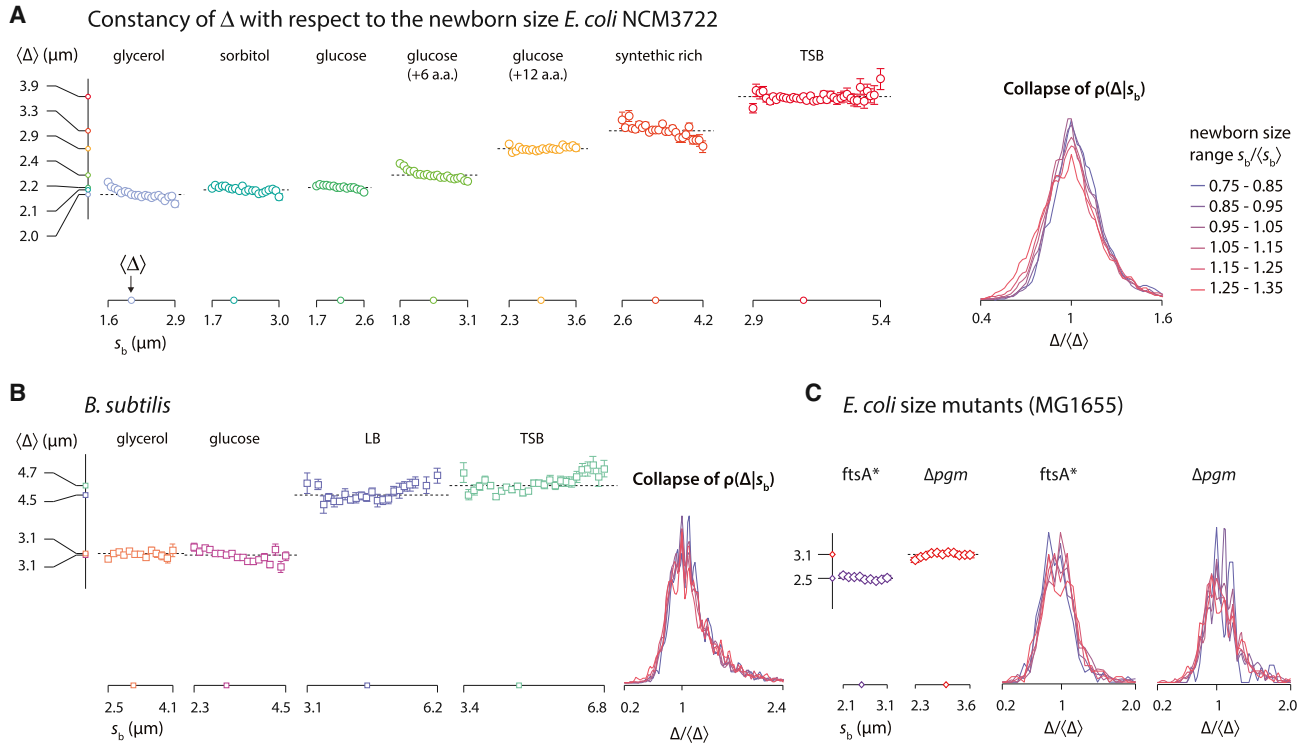

Figure 2. Experimental Evidence of Constancy of Δ in Bacteria

(A) *E. coli*: average Δ with respect to the newborn size s_b, with each bin containing >10^3 cells.

(B and C) *B. subtilis* (B) and *E. coli* size mutants (C). All rescaled distributions conditional to different newborn size ranges collapse onto one another, demonstrating that *E. coli* and *B. subtilis* cells grow by a constant size for division, independent of the newborn cell size.

See also Figures S2 and S3.

"timer" or "sizer"). Next, we explain quantitatively consequences of this adder principle on cell-size homeostasis.

Adder Ensures Size Homeostasis

An immediate consequence of addition of constant Δ is that it automatically ensured size homeostasis because at every cell division, the cell approached (albeit passively) the population average as illustrated in Figure 3A (data depict the average behavior in all growth conditions). If a cell born at size $s_b = \langle s_b \rangle + \delta s_b$ stochastically added an uncorrelated size Δ and divided in the middle with some precision, then the daughter sizes on average were $\langle s_b \rangle + \delta s_b/2$. After *n* consecutive divisions, the original size deviation of the newborn cell on average decreased as $\delta s_b/2^n$ (Figure 3A). The size homeostasis principle was confirmed by our data for both *E. coli* and *B. subtilis* (Figures 3B and 3C).

Addition of Constant Size and Exponential Elongation Explain Correlations

The constant Δ model predicted that autocorrelations of s_b, s_d, and τ_d decayed by a factor of two in each generation and that the correlation coefficient between the generation time of the mother and its daughters was −1/4, which was also confirmed by the data (Figure S4). Intuitively, the negative correlation reflects the increased generation time of the daughter cells that were born smaller than s_b due to stochastic, premature division of the mother cell [4]. Since all cells elongated exponentially with the elongation rate proportional to the cell length, cells born at $s_b < \langle s_b \rangle$ would require more time to elongate by Δ for division than cells born at $s_b > \langle s_b \rangle$ (Figure 1D, left, dashed line).

Distributions of the Growth and Division Parameters Collapse when Rescaled by Their Respective Means

The constant Δ model in fact provides a quantitative explanation for the distributions of quantities involved in growth and size control. The six distributions of the relative septum position $s_{1/2}$, elongation rate α, division size s_d, newborn size s_b, generation time τ_d, and size increment Δ are shown in Figure 4A. The coefficients of variation (CVs) of four distributions are related in the Δ model as

$$\left(\frac{\sigma_\Delta}{\langle\Delta\rangle}\right)^2 \approx \frac{1}{\ln 2}\left(\frac{\sigma_\tau}{\langle\tau\rangle}\right)^2 \approx 3\left(\frac{\sigma_b}{\langle s_b\rangle}\right)^2 \gtrsim 3\left(\frac{\sigma_d}{\langle s_d\rangle}\right)^2, \quad \text{(Equation 1)}$$

where σ denotes the SD of the distribution (see theory section in Supplemental Information for details). This predicted hierarchy of variability was confirmed by our data for both *E. coli* and *B. subtilis* (Figure 4B). Note that the size at birth s_b was slightly more variable than the size at division s_d because of the small variability of the septum position $s_{1/2}$. The elongation rate α was subject to its own physiological control and variability and showed negligible correlations with the distributions determined by Δ (Supplemental Information).

The constancy of Δ was finally supported by the scale invariance of the distributions shown in Figure 4A. In the constant Δ model, the average of the three size variables are related as $\langle\Delta\rangle = \langle s_b\rangle = \langle s_d\rangle/2$ and, if $\rho(\Delta)$ shows scale invariance, the three distributions $\rho(s_b)$, $\rho(s_d)$ and $\rho(\tau_d)$ also inherit the property of scale invariance of $\rho(\Delta)$ (theory section in Supplemental Information). In support of our theoretical prediction, all experimental $\rho(\Delta)$ and other size distributions collapsed onto each

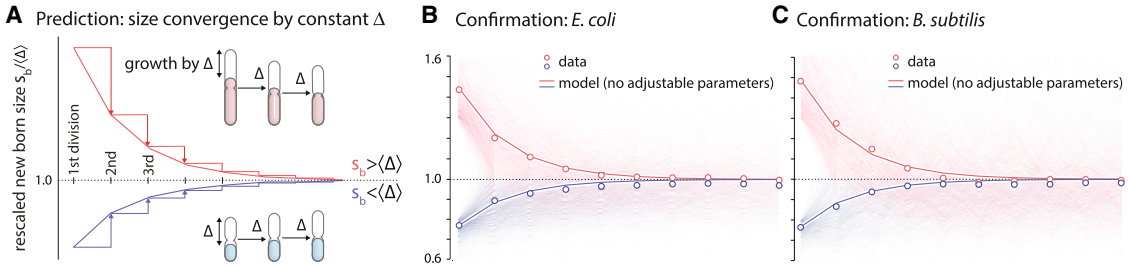

Figure 3. Mechanism of Size Homeostasis Following the Adder Principle

(A–C) For all newborn cells regardless of their size, if the cells always add a constant Δ and divide in the middle, their respective newborn size automatically converges to Δ (A). If Δ is subject to fluctuations without correlations from one generation to the next, and the cell divides in the middle with some precision, the newborn size on average still converges to $\langle\Delta\rangle$. Our data confirm this size homeostasis mechanism for both *E. coli* (B) and *B. subtilis* (C). Data in (B) and (C) show the average from all growth conditions used for each organism.

See also Movie S1.

other (Figure 4A; [23, 24]). Hence, the variation of all the statistics with growth conditions is determined by the unique parameter $\langle\Delta\rangle$.

Discussion

Proteome and Biological Origin of Constancy of Added Size

Since the proteome is a good proxy for cell size, the constant Δ is consistent with the "structural models" discussed by Fantes et al. [22]. Key features of the structural models include the following: (1) individual cells elongate exponentially, (2) initiators of cell cycle are produced at the same rate as the cell elongation rate, and (3) accumulation of the initiators to a threshold triggers the cell cycle [22]. Since the cellular volume and total number of proteins increase with the growth rate, the cellular fraction of protein initiators should reduce to maintain the constancy of the threshold. In a recent work by Scott et al. [11], the bacterial proteome is partitioned into three "sectors": R, containing ribosomal proteins; Q, containing housekeeping proteins; and P, containing the rest of the proteins. Using proteome data for the relative fraction φ_P of the P-sector proteins in *E. coli* (Figure 4E, left; [11]) and the respective average cell volume $\langle V\rangle$ (Figure 1C, red line), we found that the total number of P-sector proteins per cell $N_P = \varphi_P \times \langle V\rangle$ is relatively constant in all growth conditions for different *E. coli* strains (see Figure 4 and Supplemental Information). Thus, proteins in the P sectors behave as the initiators postulated in [22]. This leads to the prediction that the majority of proteins involved in metabolism (e.g., nutrient transporters and metabolic sensors [15]) and the cell cycle should belong to the P sector of the bacterial proteome (with their constant basal level to the Q sector). Note that the total proteome per cell increases exponentially with respect to the average growth rate; the growth law ([5]; Figure 1C) can thus be interpreted as a response of the average cell size (total proteome per cell) to nutrient conditions such that the average P-sector proteins per cell is approximately constant with respect to the nutrient-imposed growth rate. There is a clear experimental avenue for the future that will investigate how Δ will change when the proteome composition is perturbed by, e.g., transcription or translational inhibitors.

Extension to Other Organisms

The growing number of modern single-cell data sets provides a unique opportunity to determine the applicability of our findings to other bacteria as well as to eukaryotes. Analysis of bacteria, such as *Caulobacter* [25, 26], and single-celled eukaryotes should illuminate the role played by programmed degradation of regulatory proteins in cell-size homeostasis. Fantes [27] considered structural models for fission yeast *S. pombe* and dismissed them based on existing data sets. While differences might indeed be expected between eukaryotes and bacteria, extensive modern single-cell data sets are now available in, e.g., budding yeast [28], and could be used to address the question [26]. It will also be of great interest to determine whether other non-rod-shaped organisms, particularly those that exhibit tip growth and/or nonuniform morphologies, including mycobacteria, hyphal fungi, and protists like *Stentor*, also add constant volume or maintain their size through other independent mechanisms. We finally remark that the size and the shape of cells play a major role in their physiology in multicellular organisms as well, namely during *Xenopus* embryogenesis [29].

Hierarchy of Growth Parameters and the Meaning of Biological Noise

We showed that only two parameters, the elongation rate α and the added size Δ, are sufficient to reproduce the distributions of all growth and division parameters of both *E. coli* and *B. subtilis* in all growth conditions without any adjustable parameters (Equation 1 and Figure 4C; Supplemental Information). We thus propose that α and Δ represent two basic controls of physiology and size homeostasis and that the size at birth and division, as well as generation time, are slaved to them.

Ordering the variances of the rescaled distributions, the distribution of the septum position $s_{1/2}$ is the smallest, and the added size Δ is the largest (Figure 4A). Previously, sizer was supported because the coefficient of variance for division size (10%) was smaller than that for generation time (40%–60%) [19]. Therefore, interpreting coefficient of variance as a biological "noise" should be taken with caution since Δ is a basic control parameter for size homeostasis, yet Δ shows the largest variability.

Conclusions

We demonstrated that both *E. coli* and *B. subtilis* maintain cell-size homeostasis by adding a constant size Δ. The constant Δ model quantitatively explains the distributions of growth-related parameters and their variability. How bacteria can overlap their cell cycles without making fatal mistakes in the absence of eukaryotic-like cell-cycle checkpoints is a long-standing open question [30, 31]. Our results provide a new

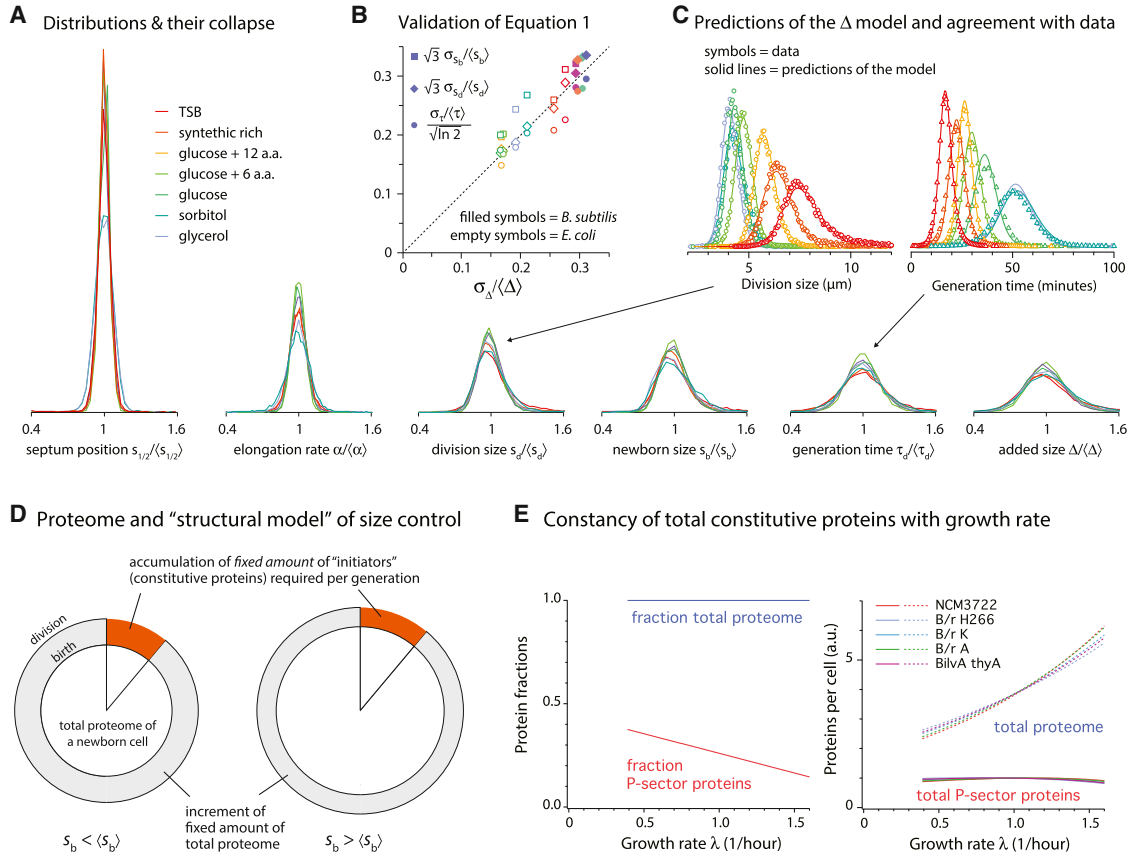

Figure 4. Origin and Quantitative Consequences of Constancy of Added Size Δ

(A) Six distributions are shown in the ascending order of their relative widths. All growth parameters from different growth conditions show scale invariance, i.e., collapse when rescaled by their respective means.

(B and C) Among the six distributions in (A), four distributions are determined by Δ (division size s_d, newborn size s_b, generation time τ_d, and Δ) (B). See Equation 1. Thus, $\rho(\Delta)$ and $\rho(\alpha)$ are sufficient to reproduce all distributions for all growth conditions for both *E. coli* (C) and *B. subtilis* (Supplemental Information) without any adjustable parameters.

(D and E) Constant Δ is consistent with the "structural models" discussed in [22], which assume that the cell grows to accumulate fixed amounts of cell-cycle regulators in each generation. Since metabolism and cell-cycle proteins are neither housekeeping nor ribosomal proteins, this prediction can be quantitatively tested using the proteome data [11] and the growth law in Figure 1C. Indeed, the total P-sector proteins per cell is constant in all growth conditions (E). See also Figure S4 and Table S3.

perspective on this issue and in the search for the underlying molecular mechanisms. A direction to be pursued in the future is the constancy of the added size Δ and its relationship with the proteome [11]. That hints at an ensemble of molecular players and entails both exponential dependency of the average cell size on growth rate (the growth law) and constancy of Δ at steady state. It will thus be important to interfere with protein synthesis and assess the resulting effects on the cell-size distributions.

Experimental Procedures

Strains

For physiological study, it is important to use a prototrophic strain. For *E. coli*, we chose the strain K12 NCM3722, constructed, sequenced, and extensively tested by Sydney Kustu's laboratory [32]. We used SJ202, a nonmotile derivative of NCM3722 (ΔmotA). For *B. subtilis* experiments, we chose a strain in the 3610 background with ComI (Q12L) mutation to allow competence. We used a derivative with reduced motility and biofilm formation by deleting *epsH* and a flagellin protein hag, respectively.

Growth Media

E. coli growth experiments were performed in seven different nutrient conditions. The average generation time in these conditions evenly spanned from 17.1 to 51.4 min at 37°C. The growth medium is based on MOPS, developed by Fred Neidhardt [33], and is commercially available from Teknova (http://www.teknova.com). *B. subtilis* growth experiments were performed in four different growth conditions with average doubling times between 16.9 and 38.9 min. The details of the growth media are listed in Tables S1 and S2. Prior to growth of the cells in the microfluidics device, all cultures were grown in a 37°C water bath shaker, shaking at 240 rpm.

Sample Preparations

All experimental steps—from inoculation to imaging—were performed at 37°C ± 0.1°C. To this end, all equipment was stationed in a 5′ × 7′ environmental chamber to eliminate any side effect of temperature fluctuations in the cell growth and physiology. Within the chamber, the temperature distribution was homogeneous, with forced air circulation within ±0.1°C, and constantly monitored at multiple locations. See Supplemental Information for more information.

Microscopy

Image acquisition and analysis were performed with an inverted microscope (Nikon Ti-E) equipped with Perfect Focus (PFS 3), a 100× oil immersion objective lens (NA 1.45), and white LED transmission light (TLED, Sutter Instruments, 400–700 nm), and an Andor NEO sCMOS camera was used for phase-contrast imaging. The illumination condition was 50 ms exposure with illumination intensity set at 10% of the maximum TLED intensity. The frequency of the time-lapse imaging was chosen such that about 20 or

more images were taken per generation time. Imaging in phase contrast eliminated potential artifacts common in fluorescence imaging. Analysis of the large number of phase-contrast images required development of custom high-throughput image analysis software as described in Supplemental Information.

Model for the Δ Control

We denote by s the cell size along the elongating axis of the rod and by s_b and s_d the size of cells at birth and division. We assume the width of the cell is roughly constant. If s(t) is the size of a cell at the current time t, its added size is denoted $\Delta(t) = s(t) - s_b$. The Δ model posits that the mechanism of control involves the single variable, $\Delta = s_d - s_b$, the size added between birth and division. The density of cells $n(s, \Delta', t)$ having size s and added size Δ', with g(s) = ds/dt, obeys the continuity equations

$$\partial_t n(s,\Delta',t) + \partial_s\left[g(s)n(s,\Delta',t)\right] + \partial_{\Delta'}\left[g(s)n(s,\Delta',t)\right] = -\gamma(\Delta')g(s)n(s,\Delta',t); \quad \text{(Equation 2)}$$

$$g(s)n(s,0,t) = 4g(2s)\int_0^\infty \gamma(x)n(2s,x,t)dx. \quad \text{(Equation 3)}$$

The left-hand side in Equation 2 is the total time derivative, and the two drift terms are due to the elongation of the cells, i.e., ds/dt = g(s) and dΔ(t)/dt = g(s). The right-hand side accounts for the division of cells. The Poissonian splitting rate function γ(Δ) is related to the distribution $\rho_{\Delta d}(\Delta)$ for the size added at division of individual cells as $\rho(\Delta) = \gamma(\Delta)\exp(-\int\gamma(x)dx)$. Indeed, the exponential term is the probability that the cell will not divide up to Δ and γ(Δ)dΔ is the probability of division in the range (Δ, Δ + dΔ). Simple algebra leads then to

$$\gamma(\Delta) = \frac{\rho_{\Delta d}(\Delta)}{1 - \int_0^\Delta dx \rho_{\Delta d}(x)}. \quad \text{(Equation 4)}$$

The conversion of the rate of division to unit time involves the Jacobian |dΔ(t)/dt| = g(s) that appears in the right-hand side of Equation 2. Finally, Equation 3 is the boundary condition that accounts for cells having all Δ = 0 at birth, irrespective of their size 2s at division.

Equation 2 goes back at least to [34, 35], and the formalism was then expanded and utilized for the sizer, the timer, and their combinations in a series of papers and books (see, e.g., [8, 24, 36–39]). We took the pragmatic approach of extracting the functions g and γ from the distribution of the sizes at division and of the elongation rates and using them to simulate the cell-size control process at the level of individual cells. We then compared statistical observables alternative to those used for the calibration of the model. As detailed in the Supplemental Information, this procedure allowed us to rule out timer and sizer models and to establish the consistency of the Δ model.

Supplemental Information

Supplemental Information includes Supplemental Experimental Procedures, four figures, three tables, and one movie and can be found with this article online at http://dx.doi.org/10.1016/j.cub.2014.12.009.

Author Contributions

J.P., M.V., and S.J. designed the research; S.T.-A., S.B., J.T.S., N.S.H., P.A.L., M.V., and S.J. performed the research; and S.T.-A., S.B., J.P., M.V., and S.J. wrote the paper. S.T.-A. and S.B. contributed equally to this work.

Acknowledgments

This work was supported by the Paul G. Allen Foundation, the Pew Charitable Trusts, and the National Science Foundation CAREER Award (to S.J.) and by the NIH grant GM 64671 (to P.A.L.).

Received: October 24, 2014
Revised: November 23, 2014
Accepted: December 2, 2014
Published: December 24, 2014

References

1. Schaechter, M., Maaløe, O., and Kjeldgaard, N.O. (1958). Dependency on medium and temperature of cell size and chemical composition during balanced grown of Salmonella typhimurium. J. Gen. Microbiol. *19*, 592–606.
2. Cooper, S., and Helmstetter, C.E. (1968). Chromosome replication and the division cycle of *Escherichia coli* B/r. J. Mol. Biol. *31*, 519–540.
3. Donachie, W.D. (1968). Relationship between cell size and time of initiation of DNA replication. Nature *219*, 1077–1079.
4. Koch, A.L., and Schaechter, M. (1962). A model for statistics of the cell division process. J. Gen. Microbiol. *29*, 435–454.
5. Powell, E.O. (1964). A note on Koch & Schaechter's hypothesis about growth and fission of bacteria. J. Gen. Microbiol. *37*, 231–249.
6. Sompayrac, L., and Maaloe, O. (1973). Autorepressor model for control of DNA replication. Nat. New Biol. *241*, 133–135.
7. Voorn, W.J., Koppes, L.J., and Grover, N.B. (1993). Mathematics of cell division in *Escherichia coli*: comparison between sloppy-size and incremental-size kinetics. Current Topics in Mol. Genet. *1*, 187–194.
8. Osella, M., Nugent, E., and Cosentino Lagomarsino, M. (2014). Concerted control of *Escherichia coli* cell division. Proc. Natl. Acad. Sci. USA *111*, 3431–3435.
9. Amir, A. (2014). Cell size regulation in bacteria. Phys. Rev. Lett. *112*, 208102.
10. Son, S., Tzur, A., Weng, Y., Jorgensen, P., Kim, J., Kirschner, M.W., and Manalis, S.R. (2012). Direct observation of mammalian cell growth and size regulation. Nat. Methods *9*, 910–912.
11. Scott, M., Gunderson, C.W., Mateescu, E.M., Zhang, Z., and Hwa, T. (2010). Interdependence of cell growth and gene expression: origins and consequences. Science *330*, 1099–1102.
12. Mitchison, J., and Werner, D. (1977). Mitosis Facts and Questions: Proceedings in Life Sciences, M. Little, N. Paweletz, C. Petzelt, H. Ponstingl, D. Schroeter, and H.-P. Zimmermann, eds. (Berlin: Springer), pp. 1–19.
13. Fantes, P.A., and Nurse, P. (1981). Division timing: controls, models and mechanisms. In The Cell Cycle, P.C.L. John, ed. (Cambridge: Cambridge University Press), pp. 11–34.
14. Kafri, R., Levy, J., Ginzberg, M.B., Oh, S., Lahav, G., and Kirschner, M.W. (2013). Dynamics extracted from fixed cells reveal feedback linking cell growth to cell cycle. Nature *494*, 480–483.
15. Weart, R.B., Lee, A.H., Chien, A.C., Haeusser, D.P., Hill, N.S., and Levin, P.A. (2007). A metabolic sensor governing cell size in bacteria. Cell *130*, 335–347.
16. Hill, N.S., Kadoya, R., Chattoraj, D.K., and Levin, P.A. (2012). Cell size and the initiation of DNA replication in bacteria. PLoS Genet. *8*, e1002549.
17. Wold, S., Skarstad, K., Steen, H.B., Stokke, T., and Boye, E. (1994). The initiation mass for DNA replication in *Escherichia coli* K-12 is dependent on growth rate. EMBO J. *13*, 2097–2102.
18. Bates, D., and Kleckner, N. (2005). Chromosome and replisome dynamics in *E. coli*: loss of sister cohesion triggers global chromosome movement and mediates chromosome segregation. Cell *121*, 899–911.
19. Schaechter, M., Williamson, J.P., Hood, J.R., Jr., and Koch, A.L. (1962). Growth, cell and nuclear divisions in some bacteria. J. Gen. Microbiol. *29*, 421–434.
20. Helmstetter, C.E., and Cummings, D.J. (1963). Bacterial synchronization by selection of cells at division. Proc. Natl. Acad. Sci. USA *50*, 767–774.
21. Wang, P., Robert, L., Pelletier, J., Dang, W.L., Taddei, F., Wright, A., and Jun, S. (2010). Robust growth of *Escherichia coli*. Curr. Biol. *20*, 1099–1103.
22. Fantes, P.A., Grant, W.D., Pritchard, R.H., Sudbery, P.E., and Wheals, A.E. (1975). The regulation of cell size and the control of mitosis. J. Theor. Biol. *50*, 213–244.
23. Trueba, F.J., Neijssel, O.M., and Woldringh, C.L. (1982). Generality of the growth kinetics of the average individual cell in different bacterial populations. J. Bacteriol. *150*, 1048–1055.
24. Giometto, A., Altermatt, F., Carrara, F., Maritan, A., and Rinaldo, A. (2013). Scaling body size fluctuations. Proc. Natl. Acad. Sci. USA *110*, 4646–4650.
25. Iyer-Biswas, S., Wright, C.S., Henry, J.T., Lo, K., Burov, S., Lin, Y., Crooks, G.E., Crosson, S., Dinner, A.R., and Scherer, N.F. (2014). Scaling laws governing stochastic growth and division of single bacterial cells. Proc. Natl. Acad. Sci. USA *111*, 15912–15917.
26. Jun, S., and Taheri-Araghi, S. (2014). Cell-size maintenance, universal strategy revealed. Trends Microbiol. Published online December 11, 2014. http://dx.doi.org/10.1016/j.tim.2014.12.001.
27. Fantes, P.A. (1977). Control of cell size and cycle time in *Schizosaccharomyces pombe*. J. Cell Sci. *24*, 51–67.

28. Di Talia, S., Skotheim, J.M., Bean, J.M., Siggia, E.D., and Cross, F.R. (2007). The effects of molecular noise and size control on variability in the budding yeast cell cycle. Nature *448*, 947–951.
29. Good, M.C., Vahey, M.D., Skandarajah, A., Fletcher, D.A., and Heald, R. (2013). Cytoplasmic volume modulates spindle size during embryogenesis. Science *342*, 856–860.
30. Mitchison, J.M. (1972). The Biology of the Cell Cycle (Cambridge: Cambridge University Press).
31. Marshall, W.F., Young, K.D., Swaffer, M., Wood, E., Nurse, P., Kimura, A., Frankel, J., Wallingford, J., Walbot, V., Qu, X., and Roeder, A.H.K. (2012). What determines cell size? BMC Biol. *10*, 101.
32. Soupene, E., van Heeswijk, W.C., Plumbridge, J., Stewart, V., Bertenthal, D., Lee, H., Prasad, G., Paliy, O., Charernnoppakul, P., and Kustu, S. (2003). Physiological studies of *Escherichia coli* strain MG1655: growth defects and apparent cross-regulation of gene expression. J. Bacteriol. *185*, 5611–5626.
33. Neidhardt, F.C., Bloch, P.L., and Smith, D.F. (1974). Culture medium for enterobacteria. J. Bacteriol. *119*, 736–747.
34. Collins, J.F., and Richmond, M.H. (1962). Rate of growth of *Bacillus cereus* between divisions. J. Gen. Microbiol. *28*, 15–33.
35. Tyson, J.J., and Diekmann, O. (1986). Sloppy size control of the cell division cycle. J. Theor. Biol. *118*, 405–426.
36. Diekmann, O., Lauwerier, H., Aldenberg, T., and Metz, J. (1983). Growth, fission and the stable size distribution. J. Math. Biol. *18*, 135–148.
37. Perthame, B. (2007). Transport Equations in Biology (Basel: Birkhäuser Verlag).
38. Wheals, A.E. (1982). Size control models of *Saccharomyces cerevisiae* cell proliferation. Mol. Cell. Biol. *2*, 361–368.
39. Robert, L., Hoffmann, M., Krell, N., Aymerich, S., Robert, J., and Doumic, M. (2014). Division in *Escherichia coli* is triggered by a size-sensing rather than a timing mechanism. BMC Biol. *12*, 17.

Update

Current Biology
Volume 27, Issue 9, 8 May 2017, Page 1392

DOI: https://doi.org/10.1016/j.cub.2017.04.028

CellPress

Current Biology
Correction

Cell-Size Control and Homeostasis in Bacteria

Sattar Taheri-Araghi, Serena Bradde, John T. Sauls, Norbert S. Hill, Petra Anne Levin, Johan Paulsson, Massimo Vergassola,* and Suckjoon Jun*

*Correspondence: massimo@physics.ucsd.edu (M.V.), suckjoon.jun@gmail.com (S.J.)

http://dx.doi.org/10.1016/j.cub.2017.04.028

(Current Biology *25*, 385–391; February 2, 2015)

We have become aware of an error in Equation 1 and Figure 4B of this article. The corrected Equation 1 should read as follows, to match Equation 25 in the Supplemental Information, which presents a full derivation of the correct Equation 1 without the error:

$$\left(\frac{\sigma_\Delta}{\langle\Delta\rangle}\right)^2 \approx 3\cdot \ln 2^2 \left(\frac{\sigma_\tau}{\langle\tau\rangle}\right)^2 \approx 3\left(\frac{\sigma_b}{\langle s_b\rangle}\right)^2 \gtrapprox 3\left(\frac{\sigma_d}{\langle s_d\rangle}\right)^2. \qquad \text{(Equation 1)}$$

Figure 4B with a corrected annotation is shown below. The data in Figure 4B remain unchanged.

Please note that these errors do not impact the results of our study. The authors apologize for any confusion.

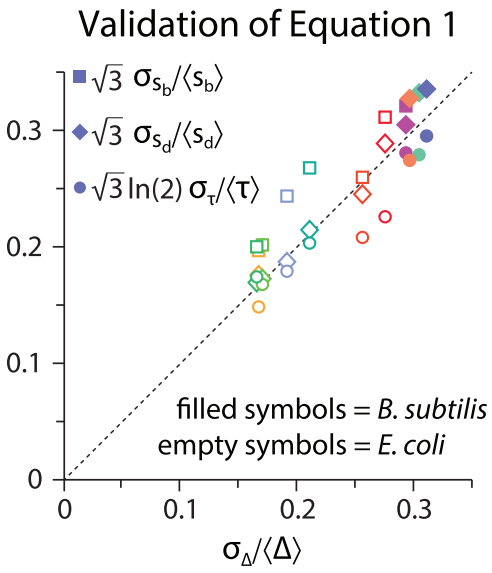

Figure 4B. Origin and Quantitative Consequences of Constancy of Added Size Δ